IX. PLASMA PHYSICS*

Prof. S. C. Brown
Prof. G. Bekefi
Prof. K. U. Ingard
Prof. D. R. Whitehouse
Dr. J. C. Ingraham
M. L. Andrews
V. Arunasalam
C. D. Buntschuh
J. F. Clarke
J. D. Coccoli
F. X. Crist
E. W. Fitzgerald, Jr.
K. W. Gentle
W. H. Glenn, Jr.
E. B. Hooper, Jr.
P. W. Jameson
R. L. Kronquist
D. T. Llewellyn-Jones
J. J. McCarthy
W. J. Mulligan
J. J. Nolan, Jr.
H. R. Radoski
G. L. Rogoff
F. Y-F. Tse
R. E. Whitney

A. ELECTRON-ENERGY DECAY IN THE HELIUM AFTERGLOW

A study of the electron-energy decay in the afterglow of a pulsed dc discharge in helium has been carried out. The electron energy is determined from the microwave power emitted from the plasma by using techniques similar to those of Bekefi and Brown[1] for steady-state electron-energy measurements and of Formato and Gilardini,[2] and Stotz and Holt[3] for transient electron-energy measurements.

1. Experiment

The pulsed dc discharge was produced in a 13 mm × 15 mm quartz tube of 75-cm length by passing a current ranging from 10 ma to 1200 ma through the tube for approximately 500 μsec at a repetition rate of 200 sec^{-1}. Helium pressures of 0.03-2.0 mm Hg were used in the experiments. Part of the discharge tube length was contained inside a 1 in. × 2 in. waveguide in such a manner that the tube and waveguide axes were nearly coincident. The discharge tube was mounted on the axis of a solenoid magnet that produced a magnetic field uniform to 1 per cent over the length of the discharge within the waveguide.

The microwave radiation detector consisted of a 5500-mc local oscillator, a balanced crystal mixer, and a 30-mc IF amplifier of 10-mc bandwidth. Through control of the IF amplifier with a 1-μsec gating signal, the time resolution necessary for transient temperature measurements was achieved in the experiment. Making the transient process periodic through repetitive pulsing of the plasma and integrating the measurement over many pulses yielded an instrumental accuracy of approximately ±100°K over the temperature range 300°-20,000°K.[4]

The longitudinal magnetic field that could be applied to the plasma served to minimize the electron particle and energy decay in the afterglow arising from diffusion to

*This work was supported in part by the U.S. Atomic Energy Commission (Contract AT(30-1)-1842); and in part by the U.S. Air Force (Electronic Systems Division) under Contract AF19(604)-5992.

the walls. Also, by maintaining the magnetic field near the value corresponding to cyclotron resonance of the electrons at the frequency at which the microwave radiation was observed (5530 mc), the absorption, and hence emission of the plasma, was increased, thereby increasing the effective signal that was measured. The magnetic field was especially necessary at pressures below 0.75 mm Hg.

The temperature standard was a neon gas discharge calibrated by Bendix Corporation, having a radiation temperature of 18,000°K ± 680°K, and a precision attenuator. All helium gas samples were of Reagent Grade (supplied by Air Reduction Sales Company), having a typical impurity content of one part in 10^5.

2. Theory

Following the termination of the power to the discharge, the electron energy approaches room temperature as determined by the combined effect of various mechanisms acting both to decrease and increase the electron average energy.

Electron energy is removed by elastic recoil collisions between electrons of mass m and atoms or ions of mass M, for which on the average the electron loses a fraction g = 2m/M of its energy per collision. Other processes that can contribute to cooling of the electrons are inelastic collisions and diffusion cooling. The average electron energy is increased through collisions of the second kind (superelastic) with excited atoms, or through processes that produce high-energy electrons such as the ionizing collision between two helium metastable atoms.[5] Electron-ion recombination, which favors the removal of low-energy electrons, also acts to increase the average free electron energy.

The following analysis accounts only for the effect of elastic recoil cooling and metastable heating. The two cases in which either metastable-metastable ionizing collisions or electron-metastable superelastic collisions is the dominant heating mechanism of the electrons in the afterglow period are treated separately. The superelastic collision that converts the $2\,^1S$ (20.61 ev) metastable state to the $2\,^3S$ (19.82 ev) metastable state[6] in helium is not included in this analysis.

Consider first the metastable-metastable contribution to the electron heating. The Boltzmann equation is written

$$\frac{\partial f}{\partial t} = \frac{g}{2v^2}\frac{d}{dv}v^3\nu_c\left(f + \frac{kT_g}{mv}\frac{df}{dv}\right) + \left(\frac{\partial f}{\partial t}\right)_{ee} + \beta n_m^2 \frac{\delta(\epsilon-\epsilon'_m)}{4\pi\left(\frac{2}{m^3}\right)^{1/2}\epsilon'^{1/2}_m}, \qquad (1)$$

where

ν_c = electron-atom collision frequency
T_g = gas atom temperature (300°K)
n_m = metastable atom density

β = rate coefficient for metastable-metastable ionizing collisions

$\delta(\epsilon-\epsilon'_m)$ = electron source function normalized so that

$$\int_{\epsilon<\epsilon'_m}^{\epsilon>\epsilon'_m} \delta(\epsilon-\epsilon'_m)\, d\epsilon = 1$$

v = electron speed

ϵ = electron energy

ϵ'_m = energy of electrons produced by metastable atoms

f = electron velocity distribution normalized so that

$4\pi\left(\frac{2}{m^3}\right)^{1/2} \int_0^\infty f\epsilon^{1/2}\, d\epsilon = 4\pi \int_0^\infty fv^2\, dv = n$, where n is the electron particle density, assumed to be independent of position.

The first term on the right-hand side of Eq. 1 represents the electron-atom elastic recoil,[7] the second term represents the electron-electron interaction, and the third term is due to the metastable-metastable ionizing collisions.

To obtain an approximate solution to Eq. 1, the electron-energy distribution in the vicinity of the electron average energy ($\approx$1 ev) is assumed to be Maxwellian in form, but in the vicinity of ϵ'_m ($\approx$20 ev) no restriction is placed on the distribution function. Near $\epsilon = \epsilon'_m$, $\left(\frac{\partial f}{\partial t}\right)_{ee}$ is approximated by $-\frac{f - f_o}{\tau_{ee}}$, where f_o is a Maxwellian whose average energy equals the average energy of all the electrons, and τ_{ee} is the electron collision time for electrons of energy ϵ'_m given by Spitzer.[8] The elastic-recoil term in the vicinity of ϵ'_m is approximated by $-g\nu_{cm}f$. For those cases in which $\tau_{ee} \ll \tau_m/2$, where τ_m is the metastable decay time constant caused mainly by diffusion loss, an approximate solution that is valid for all electron energies can be obtained.

$$f = f_o + \frac{\tau_{ee}}{1 + g\nu_{cm}\tau_{ee}} \frac{\beta n_m^2 \delta(\epsilon-\epsilon'_m)}{\epsilon_m^{1/2}(2/m^3)^{1/2}4\pi}. \tag{2}$$

Calculating the average energy from Eq. 2 and substituting a reasonable estimate for the contribution of the second term on the right-hand side, we find that it may be neglected, and we obtain

$$\bar{\epsilon} = \frac{3}{2}kT. \tag{3}$$

The expression for the rate of change of the average electron energy is calculated by appropriate integration of Eq. 1 over all electron energies. Assuming that $\nu_c \sim v$

(as it does in helium for electron energies less than 2 ev), and making use of the fact that the integration of the electron-electron term over all energy is zero, gives

$$\frac{d\bar{\epsilon}}{dt} = -a(T/T_g)^{1/2}\frac{3}{2}k(T-T_g) + \frac{\epsilon'_m \beta n_m^2}{n(1+\tau_{ee}g\nu_{cm})}. \tag{4}$$

Here, a is a pressure-dependent constant determined by the magnitude of the electron-atom collision probability.

An analogous treatment for the case of superelastic heating, including the effect of inelastic collisions, gives for the rate of change of the average electron energy

$$\frac{d\bar{\epsilon}}{dt} = -a\left(\frac{T}{T_g}\right)^{1/2}\frac{3}{2}k(T-T_g) + \frac{8\pi}{m^2}n_m\epsilon_m\int_0^\infty \frac{\sigma_{se}\epsilon f\, d\epsilon}{1+\tau_{ee}\left(g\nu_{cm}+\sigma_{se}\epsilon\left(\frac{2}{m(\epsilon+\epsilon_m)}\right)^{1/2}N\right)}. \tag{5}$$

Here, ϵ_m is the metastable energy. The superelastic cross section σ_{se} is calculated from the measured inelastic cross section σ_i, for the excitation of the $2\,^3S$ state of helium[9] from the formula $\sigma_{se}[\epsilon-\epsilon_m] = \frac{\epsilon}{\epsilon-\epsilon_m}\sigma_i[\epsilon]$. The contribution of the $2\,^1S$ state is accounted for by assuming that its excitation function has the same shape as the $2\,^3S$ state.

The "heating terms" of Eqs. 3 and 5 can be readily calculated in the limit of strong (τ_{ee}=0) and weak (τ_{ee} large) electron-electron interaction in the vicinity of the metastable energy. For these cases we obtain:

$$H_{mm} = \frac{\beta n_m^2}{n}\epsilon'_m \tag{6}$$

$$H'_{mm} = \frac{\beta n_m^2}{n\tau_{ee}g\nu_{cm}}\epsilon'_m \tag{7}$$

$$H_{se} = n_m\epsilon_m\overline{\sigma_{se}V} \tag{8}$$

$$H'_{se} = \frac{4}{3\pi^{1/2}}\frac{n_m(3/2\ kT)}{N\tau_{ee}}\left(\frac{\epsilon_m}{kT}\right)^{3/2}. \tag{9}$$

The prime on the H denotes the weak electron-electron interaction (non-Maxwellian) case.

3. Results and Analysis

In all cases reported here the plasma radiation temperature was related to the electron average energy by the equation $\bar{\epsilon} = \frac{3}{2} kT_r$.[10] Figure IX-1 displays a typical electron temperature decay as measured in the helium afterglow at 0.520 mm pressure. Also

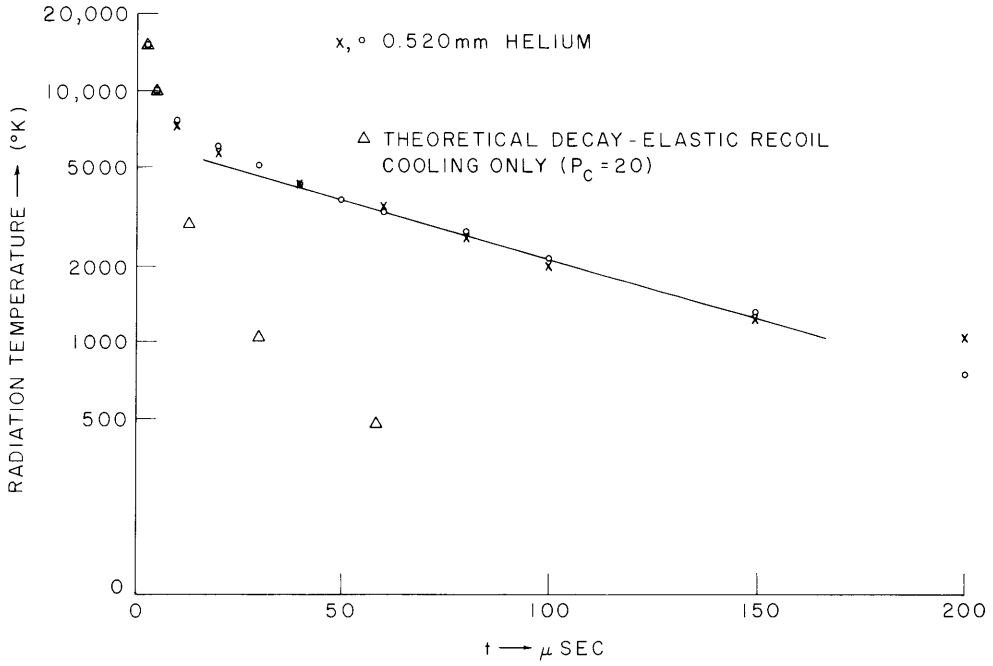

Fig. IX-1. Typical temperature decay observed in helium at 0.520-mm pressure.

plotted is the theoretical decay for elastic-recoil cooling. It is seen that there is some heating present in the afterglow.

From Eqs. 3 and 5 it can be seen that since we know the temperature as a function of time from our measurement, we can calculate the time derivative of the energy, as well as the value of the elastic-recoil term. The actual form of H is just the difference between these two terms. Also, H can be calculated by using Eqs. 6-9. Figures IX-2 and IX-3 display the time dependence of the actual form of H as calculated from the temperature-decay data as points on the graphs. Shown for comparison are the direct computations of H as determined from Eqs. 6-9. The calculation of $\overline{\sigma_{se} V}$ in Eq. 8 is done numerically by using the exact form of σ_{se} as determined from experiment.[9] Since $\tau_{ee} \sim \frac{1}{n}$, it is necessary in Eq. 9 to calculate the variation of the electron density. This is done through a numerical integration of the magneto-ambipolar diffusion equation for the electrons. In the metastable-metastable case both H_{mm} and H'_{mm} decay with the time constant $\tau_{m/2}$ because H'_{mm} is independent of electron density and in H_{mm} the

electron density may be assumed to be constant to a good approximation.[10] For the superelastic heating cases, H_{se} and H'_{se} are both plotted only when they differ sufficiently in form.

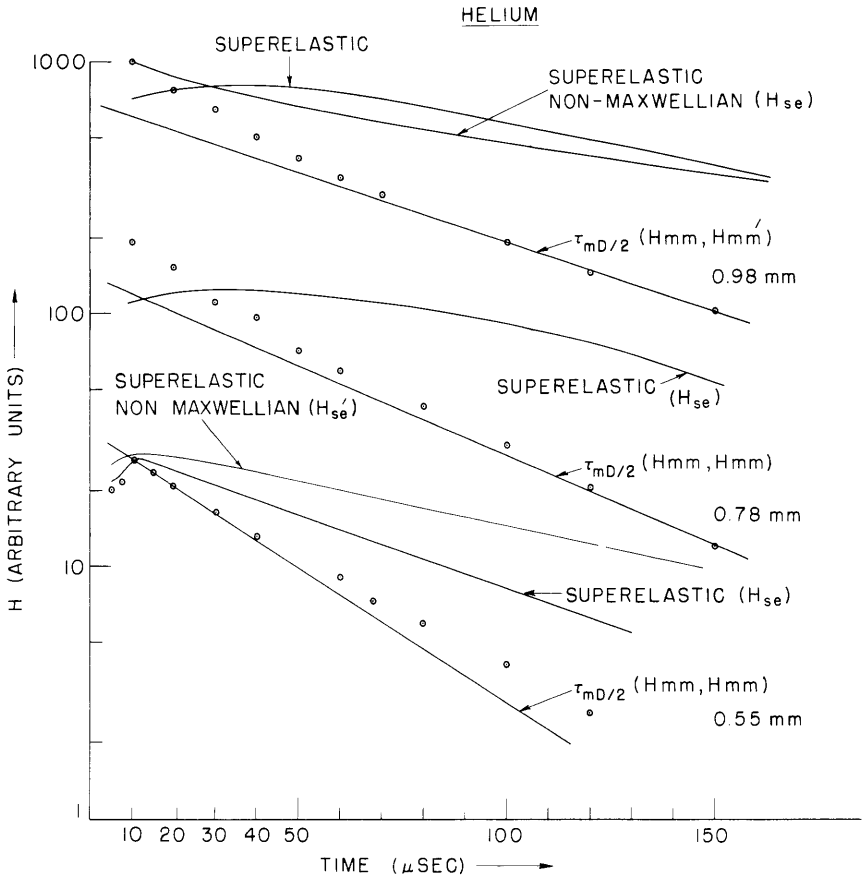

Fig. IX-2. Analysis of temperature decay for H at pressures of 0.98, 0.78, and 0.515 mm Hg in helium.

The data, when plotted in this manner, indicate that the metastable-metastable ionizing collision is the dominant heating mechanism at 1.00-mm Hg pressure, and that as the pressure is decreased, the superelastic heating becomes relatively more important, until at 0.12 mm Hg it appears to be the dominant heating mechanism. In Fig. IX-2 for pressures of 0.75 mm and 1.00 mm the experimental points fall only along the theoretical metastable-metastable heating line for times late in the afterglow. Such behavior could be due to the presence of higher diffusion modes in the metastable atom density, or to the effect (not accounted for) of the superelastic collision that converts the $2\ ^1S$ metastable state into the $2\ ^3S$ metastable state. Order-of-magnitude calculation shows that the metastable destruction resulting from metastable-metastable ionizing collisions

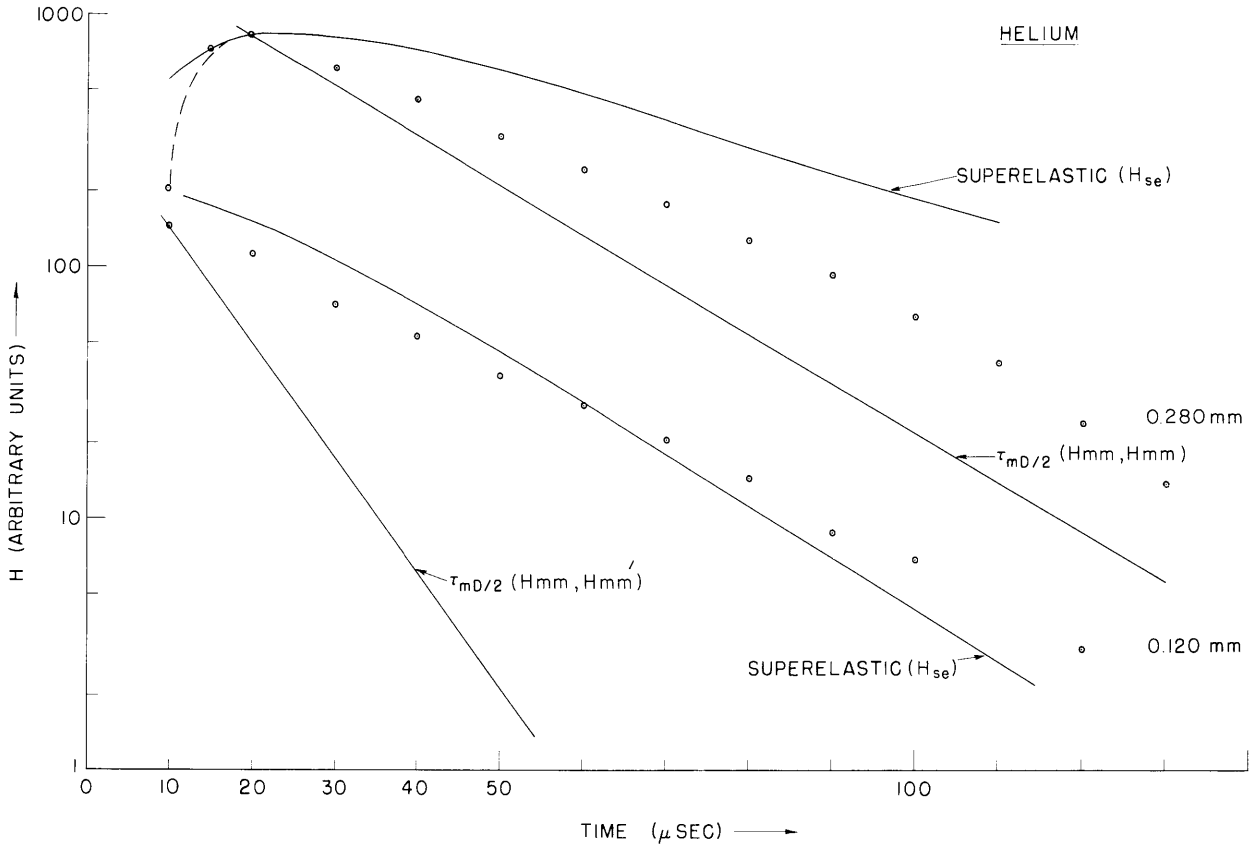

Fig. IX-3. Analysis of temperature decay for H at pressures of 0.28 and 0.12 mm Hg in helium.

is probably negligible compared with diffusion loss.

The initial metastable atom density, arising approximately from the establishment of a steady state between metastable production through electron collisional excitation of the helium gas atoms and metastable loss that is due to diffusion, will be proportional to the square of the pressure. Since the metastable-metastable heating is quadratic in the metastable density and the superelastic heating is linear, we would indeed expect the linear heating effect to become more important at the low pressures as is observed.

By using such a model it is possible to estimate the metastable density, since the rate of production of metastables can then be calculated from the known inelastic cross section σ_i and the loss rate from the known metastable diffusion coefficient. For a typical case at 1.00 mm pressure, for which the initial afterglow temperature was measured to be 40,000°K and the initial electron density estimated as 2×10^{11} cm^{-3} from the discharge current (60 ma) and voltage (350 volts), the initial metastable density is found to be $n_{m_o} = 1.9 \times 10^{13}$ cm^{-3}.

It is then possible to calculate a value for the metastable-metastable rate coefficient,

provided that we can assume that either the strongly Maxwellian or the non-Maxwellian case applies. If we choose arbitrarily the point at 100 μsec in the afterglow, where the measured temperature was 2300°K for the above-mentioned conditions, the ratios H_{mm}/H_{se} and H'_{mm}/H'_{se} can be calculated. The latter ratio is found to have the value 24.5; and the former, 0.06; these calculations indicate that the strongly non-Maxwellian case applies, since the results illustrated by Fig. IX-2 indicate that either H_{mm} or H'_{mm} is the dominant heating mechanism at 1.00-mm pressure. The value of β thus calculated under the assumption that the strong non-Maxwellian case holds is $\beta = 4 \times 10^{-11}$ cm^3 sec^{-1}.

Under the assumption that metastable-metastable heating dominated at 0.50-mm pressure, and by observing how the metastable decay rate τ_m changed with the addition to the helium of measured amounts of neon and argon, it was possible to calculate the cross sections for metastable destruction, σ_D, in neon and argon. The results were: for argon, $\sigma_D = 1.09 \pm 0.15 \times 10^{-16}$ cm^2; and for neon, $\sigma_D = 3.1 \pm 0.75 \times 10^{-17}$ cm^2. These values agree well with Biondi's[11] value for argon of $\sigma_D = 9.3 \pm 0.8 \times 10^{-17}$ cm^2 and Javan's[12] value for neon of $\sigma_D = 3.7 \pm 0.5 \times 10^{-17}$ cm^2.

We have shown that the energy decay at 1.00-mm Hg pressure is determined by cooling of the electrons resulting from electron-atom elastic-recoil collisions and heating caused by metastable-metastable ionizing collisions that produce energetic electrons. At 0.12 mm Hg, the dominant heating mechanism is electron-metastable superelastic collisions. The addition of measured amounts of impurity gases can be used as an aid in analysis, as well as a means of studying properties of the impurity gases.

J. C. Ingraham, S. C. Brown

References

1. G. Bekefi and S. C. Brown, J. Appl. Phys. 32, 25 (1961).

2. D. Formato and A. Gilardini, Proceedings of the Fourth International Conference on Ionization Phenomena in Gases (North Holland Publishing Company, Amsterdam, 1960), Vol. 1, p. 99.

3. K. C. Stotz and E. H. Holt, Bull. Am. Phys. Soc. 8, 174 (1963).

4. J. C. Ingraham and J. J. McCarthy, A transient microwave radiation pyrometer, Quarterly Progress Report No. 64, Research Laboratory of Electronics, M. I. T., January 15, 1962, pp. 76-79.

5. M. A. Biondi, Phys. Rev. 82, 453 (1951).

6. A. V. Phelps, Phys. Rev. 99, 1307 (1955).

7. W. P. Allis, Motions of Ions and Electrons, Technical Report 299, Research Laboratory of Electronics, Massachusetts Institute of Technology, June 13, 1956, p. 44.

8. L. Spitzer, Physics of Fully Ionized Gases (Interscience Publishers, Inc., New York, 1956), p. 80.

9. G. J. Schulz and R. E. Fox, Phys. Rev. 106, 1179 (1957).

10. J. C. Ingraham, Ph.D. Thesis, Department of Physics, M.I.T., 1963.

11. M. A. Biondi, Phys. Rev. 83, 653 (1951).

12. A. Javan, W. R. Bennett, Jr., and D. R. Herriot, Phys. Rev. Letters 6, 106 (1961).

B. RELAXATION RATE OF ELECTRONS TO EQUILIBRIUM

We present the results of measurements on the time taken for the electrons of a plasma to relax from an initially non-Maxwellian to a Maxwellian distribution of velocities. The measurements were made in the afterglow of a weakly ionized, pulsed dc discharge subjected to an axial magnetic field. The experiments were made in argon in a range of pressures 0.2-2 Torr, with voltage pulses of 1-msec duration, and discharge current 10-90 ma. All relaxation measurements were made within the first 30 μsec after turning off the discharge. The experiments indicate that the distribution function f(v,t) relaxes more slowly than the relaxation resulting from electron-electron collisions, and faster than that caused by elastic recoil with atoms. In addition to these measurements, the relaxation of the mean electron energy $\overline{U}$ was observed. This relaxation rate was found to be much faster than can be predicted from elastic electron-atom collisions. The detailed mechanisms by which these processes occur are not yet understood.

1. Results

The time variation of the distribution function f(v,t) was inferred from the time-resolved measurements of the microwave emission spectrum from the plasma. The technique by which f is determined from the microwave noise has been reported elsewhere.[1] It has been shown that the radiation temperature T_r defined through the ratio of the emission to the absorption coefficients,

$$\frac{j_\omega}{a_\omega} = \frac{\omega^2}{8\pi^3 c^2} kT_r(f,\omega,\omega_b,\nu_{ea}), \tag{1}$$

is a strong function of f(v), particularly at observation frequencies ω near the electron-cyclotron frequency $\omega_b = eB/m$, where B is the strength of the magnetic field. Moreover, when the plasma is weakly ionized, T_r depends on the collision frequency for momentum transfer $\nu_{ea}(v)$ for electron-atom impacts. Thus, f can be inferred from a measurement of T_r made as a function of ω (or ω_b), and from prior knowledge of $\nu_{ea}(v)$ for the gas in question.

The radiation temperature was measured with a radiometer[2] operated at a fixed frequency of 3000 mc and bandwidth of 10 mc. The instrument was gated to sample the microwave noise signal for a duration of 1 μsec. Approximately 1000 successive samples

were taken, averaged, and detected synchronously at the repetition rate of the breakdown pulses. The 1-μsec gate could sample radiation during the time of breakdown, or at any later time up to 600 μsec after breakdown was terminated. The minimum detectable noise temperature T, defined in terms of power as $P = (kT/2\pi)\Delta\omega$, was 100°K.

The radiation temperatures T_r that we report now are those from a 50-cm length section of a 100-cm length positive column, 2.5 cm in diameter, situated in an S-band waveguide. The measurements were made by setting the radiometer gate at an appropriate time during the afterglow (or during the pulse), and varying the axial magnetic field between 0 and 1500 gauss. The results for two different gas pressures are shown in Fig. IX-4. The curves labelled "zero" time were made 2 μsec before the plasma was turned off. No variations in T_r were found, however, at any time during the last 10 μsec before turning off the voltage. The times that mark the remaining curves were measured from the end of the breakdown pulse and refer to the decaying plasma.

At a given time t, the plot of T_r against ω_b exhibits a monotonically decreasing background with a peak centered at $\omega = \omega_b$ superposed on the flat spectrum. The presence

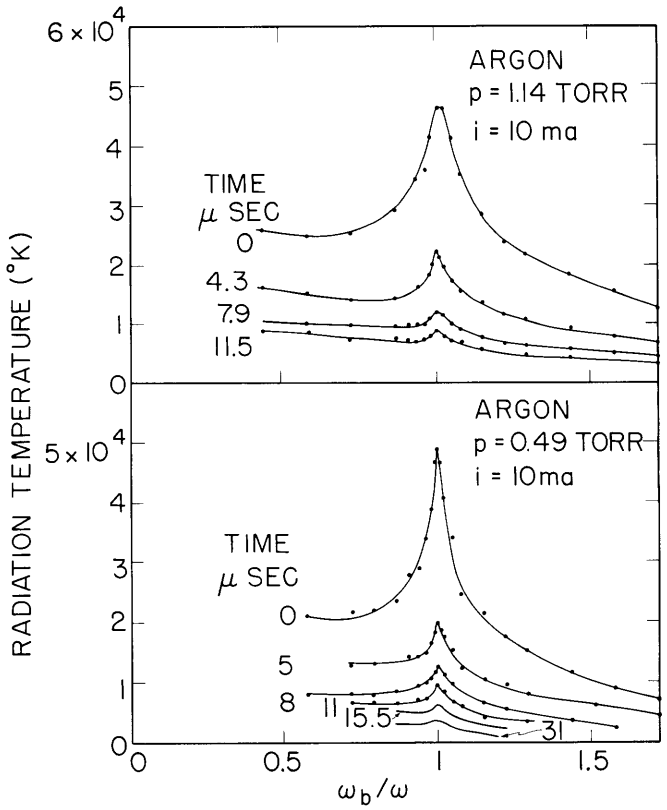

Fig. IX-4. Measured radiation temperature as a function of magnetic field at various times in the afterglow of a pulsed discharge in argon.

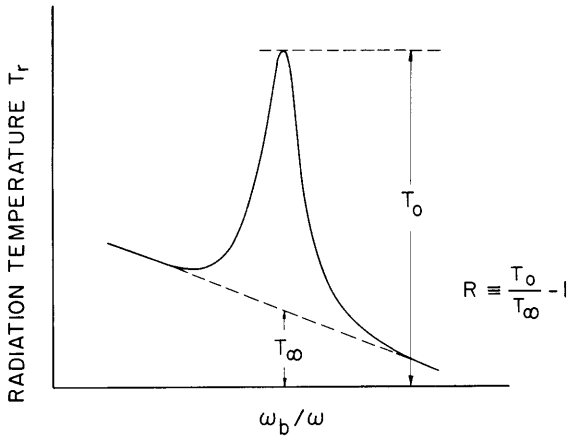

Fig. IX-5. Meaning of the relative height R of the radiation peak.

of this peak signifies that the electron distribution is not Maxwellian. Were f(v) Maxwellian, the peak would be absent; indeed, in this case, T_r would be exactly equal to the electron temperature. In the absence of a Maxwellian, no part of the curve is directly interpretable in terms of the mean electron energy $\overline{U}$, although the monotonically varying portion can be used as a rough estimate of $\overline{U}$ through $\overline{U} \approx (3/2)kT_r$.

As time progresses, we observe that the height of the peak relative to the background decreases, thereby signifying that the plasma is relaxing to a Maxwellian distribution. We also note that the background radiation temperature is falling with time, and hence that the mean electron energy $\overline{U}$ is relaxing toward the energy of the cold atoms.

A convenient measure of the rate of Maxwellianization is the relative height of the peak defined through the quantity

$$R = \frac{T_o}{T_\infty} - 1, \tag{2}$$

which is explained in Fig. IX-5. T_o is the value of the radiation temperature at $\omega = \omega_b$, whereas T_∞ is the value of the background radiation temperature extrapolated to the value for which $\omega = \omega_b$. Theory yields the following interpretation of T_∞: It is that value of T_r that would be obtained if ω_b were fixed and ω moved to very large values so that $|\omega - \omega_b| \gg \nu_{ea}$. If this could be attained experimentally, one would expect the peak to be symmetrical, and the background radiation flat and parallel to the abscissa in Fig. IX-4. The reason for the downward tilt in the spectrum is thought to be the fact that as the magnetic field increases, the value of T_r falls during the pulse ($t \leq 0$), and thus gives rise to different initial conditions for each point along the T_r versus ω_b curve.

A plot of ln R against time in the afterglow is shown in Fig. IX-6 for different currents i of the breakdown pulse. We see that R decays exponentially with time, and that the time constant for the decay (as determined from the slope of the curves) decreases as i increases. This suggests that τ is a function of electron density N, which, as a result of the large tube diameter and strong magnetic field, varies negligibly during the first 30 μsec of the afterglow. Thus we may infer N from the current density J during the pulse, and the electron drift velocity v_d by means of $J = Nev_d(E/p)$,

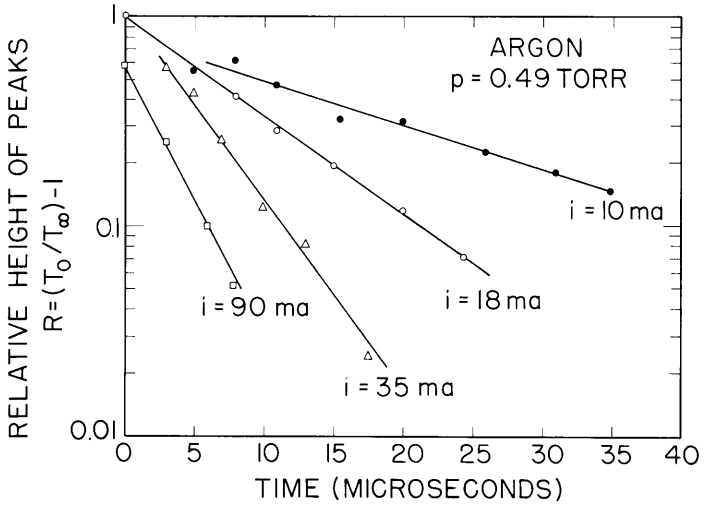

Fig. IX-6. Peak-height R(t) as a function of time in the afterglow, for different discharge currents i.

where E is the axial voltage, and p the gas pressure. In argon v_d varies almost linearly with E/p for values of $E/p \gtrsim 1$ volt cm^{-1} $Torr^{-1}$. Using the result[3]

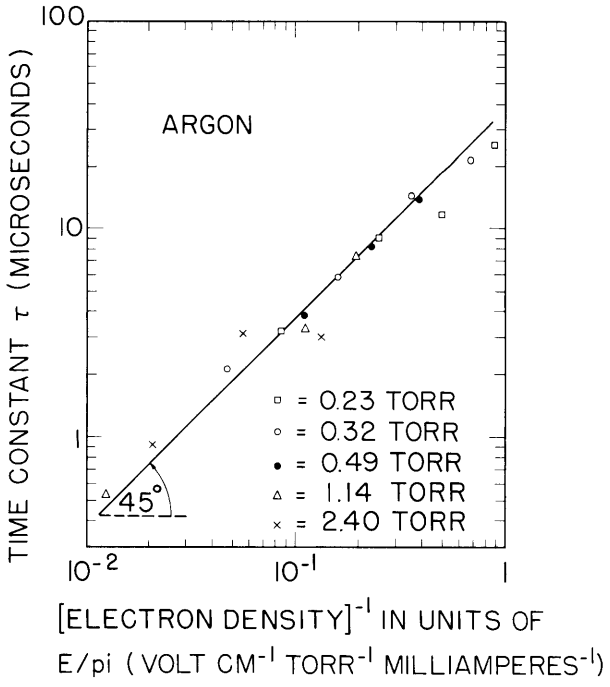

Fig. IX-7. The time constant τ of the quantity R(t) for different ratios of (E/pi).

$$v_d = 3 \times 10^5 \text{ (E/p) cm/sec,} \tag{3}$$

we obtain the following value for N averaged over the cross section of the discharge tube:

$$N = 4.2 \times 10^9 \text{ (pi/E) cm}^{-3}. \tag{4}$$

The current i is in milliamperes. Microwave cavity measurements made in the range i = 10-20 ma, p = 0.2-0.5 Torr give the value,

$$N = 3.3 \times 10^9 \text{ (pi/E) cm}^{-3}.$$

In Fig. IX-7, we show a plot of the time constant τ as a function of (E/pi) for a range of pressures 0.2-2 Torr, and currents 10-90 ma. Within the accuracy of the results τ varies inversely with N over a range close to two orders of magnitude in N; from Fig. IX-7 and Eq. 4 we find the value

$$\tau = 1.6 \times 10^5/N \text{ seconds.} \tag{5}$$

2. Discussion of Results

The relaxation of the electron distribution to a Maxwellian can pass through several processes. If inelastic collisions are neglected, there are two such processes. One comes about through energy exchange between electrons, and the other through energy exchange between electrons and the cold background gas (assumed to have a Maxwellian distribution).

The time constant for relaxation by electron-electron interactions[4] for those electrons of the distribution function which have energies $U \sim \overline{U}$ is

$$\tau_{ee} = A\left[2.59 \times 10^5 \frac{\overline{U}^{3/2}}{N \ln \Lambda}\right] \text{ seconds.} \tag{6}$$

Here $\overline{U}$ is the mean electron energy in ev, $\ln \Lambda$ is a slowly varying function of N and $\overline{U}$, and A is a numerical constant of order unity ($A \sim 1/3$ to 1). The term in brackets equals (within a factor of unity) the reciprocal of the momentum collision frequency ν_{ee} between electrons, and also the reciprocal of the momentum collision frequency ν_{ei} of electrons relaxing on ions. Equation 6 is derived under the assumption that the electrons do not collide with any other species of particle so that $\overline{U}$ is time-stationary.

The time constant for the electron-energy exchange that results from elastic recoil of electrons on neutrals is approximately

$$\tau_{ea} = \left[\frac{2m}{M}\overline{\nu}_{ea}\right]^{-1}, \tag{7}$$

where M is the mass of the atom, and $\overline{\nu}_{ea}$ is the elastic collision frequency for momentum transfer for electron-atom encounters averaged over the electron speeds. We note that even in lowly ionized plasmas, where $\nu_{ea} \gg \nu_{ei} \approx \nu_{ee}$, the relaxation of the distribution function can proceed through electron-electron collisions (Eq. 6) in preference to electron-atom collisions (Eq. 7), provided that

$$\nu_{ei} > \nu_{ea}(2m/M). \tag{8}$$

This inequality was satisfied in most of the experiments described in the previous section, a fact that first led us to think that the experimentally observed time constant τ (Eq. 5) is associated with electron-electron collisions alone. When we compare Eqs. 5 and 6 we see that one question that remains unanswered is the apparent lack of dependence of τ on energy $\overline{U}(t)$ which in our experiments continuously decreases with time. To investigate this question, we must establish the relationship between the relaxation τ of the observed quantity R(t) and the relaxation of the distribution function itself. Moreover, we need to relate the measured quantities $[T_o(t), T_\infty(t)]$ to the mean electron energy $\overline{U}(t)$.

The theoretical relationship between $T_r(t)$ and f(v,t) has been given elsewhere.[1] Numerical results were obtained under the assumption that the distribution is of the form

$$f(v,t) = B[\overline{U}(t);N] \exp[-b(t)\, v^{\ell(t)+2}], \tag{9}$$

where B, b, ℓ are positive quantities that are functions of time. The exponent $\ell(t)$ is the quantity characterizing the departure of the distribution from a Maxwellian, and we shall take its relaxation toward zero as the proper variable that describes the rate of Maxwellianization of the plasma. The justification for using the form above for f comes from the results of previous measurements on steady-state discharges.[1]

Using Eq. 9 and the known values of $\nu_{ea}(v)$ in argon, we computed T_r on a digital computer for different values of ℓ and $\overline{U}$. The results of these calculations can be expressed to a good degree of accuracy by means of the following empirical relations:

$$\ell(t) = 0.951\ R(t) \exp[0.353\, \overline{U}^{-3/2}(t)] \tag{10}$$

$$\ell(t) = 1.50[T_o(t)-\overline{U}(t)]/[\overline{U}(t)-0.460] \tag{11}$$

which are valid in the range $0 \leq \ell(t) \leq 3$, $0.4 \leq \overline{U} \leq 4$ ev. Note that a measurement of R and T_o yields ℓ and $\overline{U}$ of the distribution function (9). We now use Eq. 10 to find the rate of relaxation of $\ell(t)$. Differentiating the equation with respect to time and noting that R decays exponentially with time (as described in the previous section), we find that

$$\frac{1}{\ell}\frac{d\ell}{dt} = -\frac{1}{\tau} - \frac{0.53}{\overline{U}^{3/2}}\left[\frac{1}{\overline{U}}\frac{d\overline{U}}{dt}\right]. \tag{12}$$

We may now compare the first and second terms on the right-hand side of this equation. Let us assume, first, that $\overline{U}$ decays entirely by recoil with atoms. Then $[\overline{U}^{-1}\, d\overline{U}/dt] = \tau_{ea}^{-1}$, where τ_{ea} is given by Eq. 7. In argon $\nu_{ea} \approx 1.1 \times 10^9\, \overline{U}^{3/2} p$ (for $0.4 \leq \overline{U} \leq 8$ ev), with the result that $\tau_{ea} = [3.0 \times 10^4\, \overline{U}^{3/2} p]^{-1}$ sec. Substituting in Eq. 12, we find

$$\frac{1}{\ell}\frac{d\ell}{dt} = -\frac{1}{\tau} - [1.6 \times 10^4 p]\ \text{sec}^{-1}. \tag{13}$$

In the present experiments the second term of Eq. 13 is small compared with the first, and thus the effect of energy relaxation by elastic recoil on the decay of the distribution function is negligible. Note, however, that in an extremely tenuous plasma, the second term could outweigh the first, and then ℓ would have a time constant given by $(63/p)$ μsec.

We can show that the mean electron energy $\overline{U}$ must decay at least as fast as the quantity T_∞ defined in Fig. IX-5. An examination of the radiation data such as those in Fig. IX-4 shows that within the first 30 μsec the energy decay is much faster than that predicted above for elastic recoil alone. Also, the time constant for energy decay and the time constant τ for R(t) are not independent of one another. The details of the inelastic collision processes, which presumably give rise to the fast energy fall-off, are not understood at present.

To get a clearer idea whether electron-electron collisions are in fact responsible for the time variations of f(v,t), we make two assumptions: (a) the parameter $\ell(t)$ is the proper variable to describe the relaxation of f(v,t); and (b) the form for τ_{ee} given by Eq. 6 is valid even if $\overline{U}$ is varying rapidly. Then

$$\frac{1}{\ell}\frac{d\ell}{dt} \propto -\frac{N}{U(t)^{3/2}} \tag{14}$$

which can be written in terms of τ of Eq. 5 as

$$\frac{1}{\ell}\frac{d\ell}{dt} = -\frac{C}{\tau U(t)^{3/2}} \equiv -\frac{1}{\tau_{eff}}. \tag{15}$$

Here, τ_{eff} is the effective relaxation time, and C is a constant that we wish to determine by comparison with experiment. Equating Eqs. 12 and 15, we obtain a differential equation for $\overline{U}(t)$ whose solution is

$$[\overline{U}(t)/\overline{U}_\infty(t)]^{3/2} = [1-\{1-(\overline{U}_\infty/\overline{U}_o)^{3/2}\}\, e^{-t/\tau'}]^{-1}. \tag{16}$$

Here, $\overline{U}_o$ is the value of $\overline{U}$ at $t = 0$, $\overline{U}_\infty \equiv C^{2/3}$ is the value of $\overline{U}$ at $t \to \infty$, and the time constant τ' is given by

$$\tau' = 0.353\, \frac{\tau}{C}. \tag{17}$$

A preliminary analysis of the time variations of $\overline{U}$ was made and the results fitted to Eq. 16. Approximate agreement was obtained with $\tau' \approx \tau$. This gives a value of $C \approx 0.353$. Using this in Eq. 15 and substituting for τ from Eq. 5, we find that

$$\tau_{eff} \approx 4.5 \times 10^5 \, U(t)^{3/2}/N \text{ seconds.} \tag{18}$$

The theoretical result given by Eq. 6 gives $\tau_{ee} = A[0.26 \times 10^5 \, U^{3/2}/N]$. Here we took $\ln \Lambda = 10$, which is the value appropriate to the range of N's and $\overline{U}$'s of the experiment. We see that τ_{ee} is smaller by a factor of 20-50 as compared with τ_{eff}. This fact makes it difficult to ascribe the relaxation of f(v,t) to electron-electron collisions alone, and suggests that inelastic-collision processes, competing with electron-electron collisions, maintain the plasma as non-Maxwellian for a prolonged period of time.

G. Bekefi, H. Fields

References

1. H. Fields, G. Bekefi, and S. C. Brown, Phys. Rev. 129, 506 (1963).

2. J. C. Ingraham and J. J. McCarthy, Quarterly Progress Report No. 64, Research Laboratory of Electronics, M. I. T., January 15, 1962, pp. 76-79; J. C. Ingraham, Ph. D. Thesis, Department of Physics, M. I. T., 1963.

3. J. C. Bowe, Phys. Rev. 117, 1416 (1960).

4. J. L. Delcroix, Introduction to the Theory of Ionized Gases (Interscience Publishers, Inc., New York, 1960).

C. EFFECT OF GAS FLOW ON ELECTRICAL PROPERTIES OF A POSITIVE COLUMN

An experiment designed to study the influence of turbulence on the diffusion effects in the plasma column in a glow discharge has been set up, and some preliminary observations on the influence of gas-flow rate on the properties of the plasma column have been made.

The experimental arrangement is shown schematically in Fig. IX-8. The length of the plasma column is approximately 30 cm, and the diameter of the tube is 0.6 cm. Langmuir probes are inserted as shown in the figure. Also, hot-wire probes are used for turbulence measurements. With the present pump capacity, gas flow speeds up to sonic can be established at gas pressures of approximately 5 mm Hg, corresponding to Reynolds numbers of approximately 2000 for argon and 400 for helium. The flow rate is measured by a standard flow rate meter and is adjusted by means of a needle valve. By proper arrangement of valves, the flow rate and the gas pressure can be varied independently. The discharge tube is placed inside a magnet so that a uniform magnetic

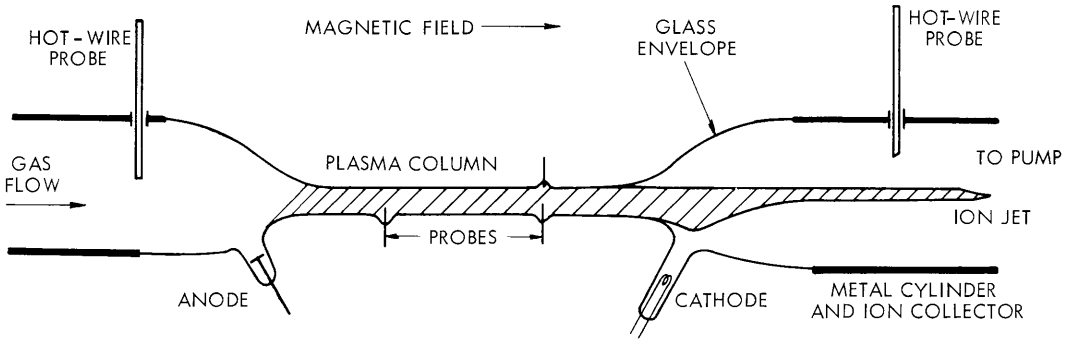

Fig. IX-8. Experimental arrangement.

field can be produced over the entire length of the plasma column.

An interesting effect of flow is that the behavior of the plasma column depends on the direction of the gas flow. When the flow goes from the cathode to the anode, the plasma column becomes striated, forming well-defined droplike luminous regions the separation of which (~1-3 cm) varies with the flow speed. This effect appears when the flow velocity is of the order of the ion drift velocity. At lower and higher speeds the striations disappear. As the flow direction is reversed, no striations are obtained; the visual appearance of the column is then almost independent of the flow rate.

With the current kept constant, the potential difference V between the Langmuir probes, separated by a distance of approximately 10 cm, has been measured as a function of the flow rate. The results depend on the direction of the flow. With the flow going from the cathode to the anode, there appears to be a minimum in the potential difference and a corresponding maximum in the conductivity, as illustrated in Fig. IX-9, which refers to measurements in argon at a pressure of 5 mm Hg. The flow rate indicated in cm^3/sec refers to a gas pressure of 5 mm Hg and room temperature. The striations of the column described above seem to occur in the neighborhood of the minima of the curves. Corresponding results when the flow goes in the reverse direction, from the anode to the cathode, are shown in Fig. IX-10. A monotonic increase of the voltage is then obtained which amounts to approximately 40 per cent at a flow rate of 100 cm^3/sec. Measurements of this kind have been made at some different gas pressures and as a function of the magnetic field. In general, the over-all influence of these variables is minor. A typical result showing the magnetic-field dependence of the potential difference V is shown in Fig. IX-11, which refers to helium at a gas pressure of 5 mm Hg and a current of 50 ma. Notice in this figure that the influence of the flow on the potential difference is somewhat increased by the magnetic field. The highest magnetic field, for 100-amp magnet current, is approximately 5000 gauss.

The mechanism responsible for the influence of the flow on the conductivity has not

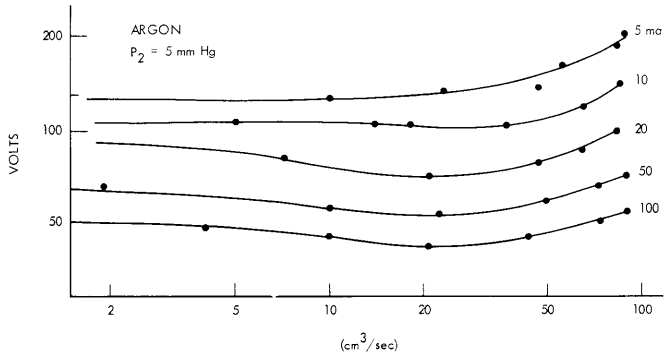

Fig. IX-9. Influence of gas flow rate on the voltage between probes in plasma column for some constant values of the discharge current. Gas flow is in the direction from the cathode to the anode.

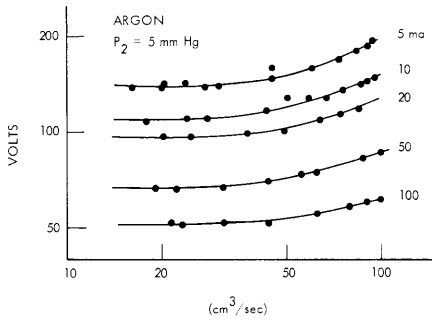

Fig. IX-10. Influence of gas flow rate on the voltage between probes in plasma column for some constant values of the discharge current. Gas flow is in the direction from the anode to the cathode.

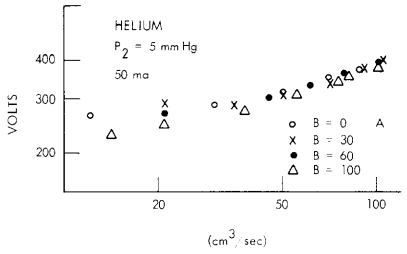

Fig. IX-11. Magnetic-field dependence of the voltage between probes in plasma column. (Magnet current 100 amps corresponds to ~3500 gauss.)

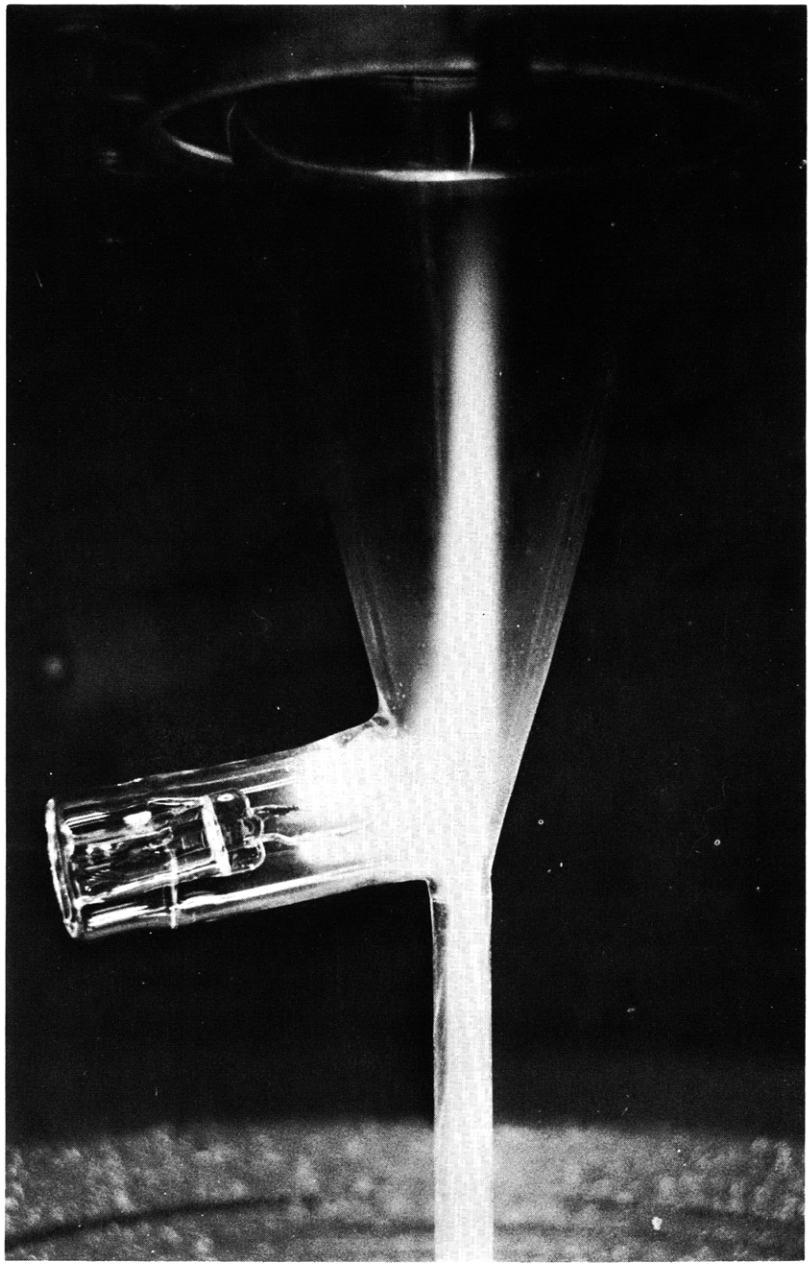

Fig. IX-12. Typical jet protruding out from discharge in argon.

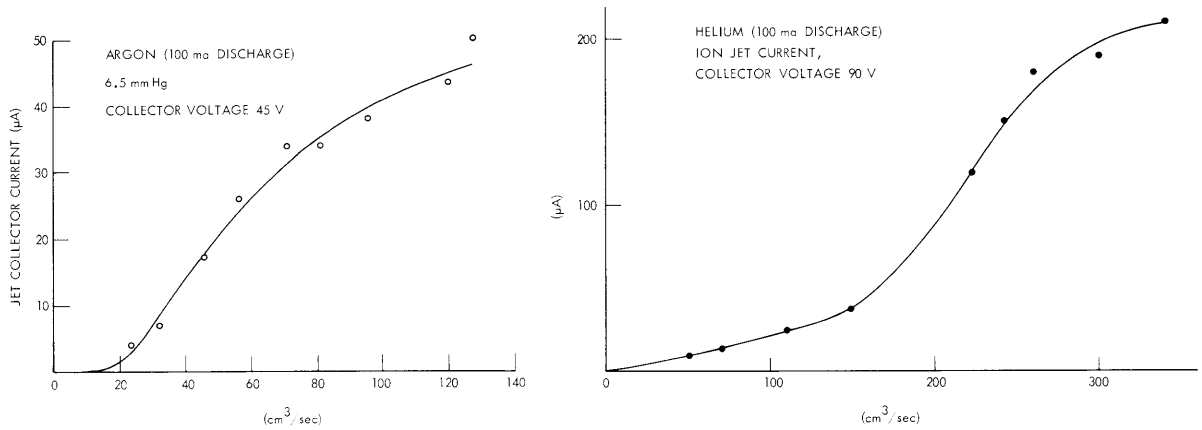

Fig. IX-13. Ion current carried by the jet shown in Fig. IX-12 as a function of the gas-flow speed.

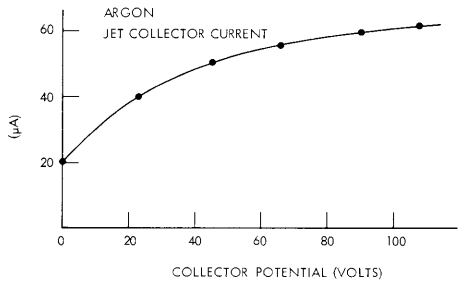

Fig. IX-14. Ion current in the jet as a function of collector voltage.

yet been established, but part of it may be connected with the removal of ions from the column by the gas jet that protrudes beyond the cathode (or anode). A typical example of such a jet is shown in Fig. IX-12, which refers to argon at a pressure of 5 mm Hg, a discharge current of 100 ma, and a flow rate of ~300 cm^3/sec. The ion current carried by this jet has been measured as a function of flow speed; typical results are shown in Fig. IX-13. The current, of course, depends on the ion collector potential, and this dependence is indicated by the curve in Fig. IX-14.

K. U. Ingard, G. Bekefi, K. W. Gentle